A planar closed-loop cable-driven parallel mechanism

H. Liu[1],   C. Gosselin[2]

[1] *Département de génie mécanique, Université Laval, Québec, Qc, hanwei.liu.1@ulaval.ca*

[2] *Département de génie mécanique, Université Laval, Québec, Qc, gosselin@gmc.ulaval.ca*

Abstract

A novel architecture of planar closed-loop cable-driven parallel mechanism is introduced in this paper. In this architecture, instead of being wound on spools, the cables form closed loops attached to the end-effector and whose motion is controlled by sliders. By eliminating the spools, it is expected that the new mechanisms will lead to a better accuracy than conventional cable-driven parallel mechanisms. This paper presents the inverse kinematics, the Jacobian matrices and the static equilibrium equations for the new architecture. Using the Jacobian matrices, the singularities of the mechanism are also analyzed. Also, based on the static equation, the available wrench set is determined. It is pointed out that the trajectory of the end-point of a given cable loop is a portion of ellipse. The intersection of the ellipses provides the assembly modes. There can be more than one intersection point of the ellipses at a given position of the sliders. This geometeric characteristic is analyzed at the end of the paper.

Keywords: cable-driven parallel mechanisms, closed-loop, kinematics, statics, singularities.

Mécanisme parallèle plan entraîné par des boucles de câbles

Résumé

Une nouvelle architecture de mécanisme parallèle plan entraîné par câbles est proposée dans cet article. Dans cette architecture, les câbles forment des boucles fermées dont le mouvement est assuré par des glissières plutôt que de s'enrouler sur des tambours comme dans une architecture conventionnelle. En éliminant les enrouleurs, on s'attend à ce que la précision du mécanisme puisse être améliorée. Cet article présente la solution au problème géométrique inverse, la dérivation des matrices jacobiennes et l'obtention des équations d'équilibre statique. Les singularités sont aussi analysées et l'ensemble des torseurs disponibles à la plate-forme est déterminé. L'analyse du mécanisme révèle que la trajectoire du point extrême d'une boucle de câble décrit une portion d'ellipse et que les intersections des ellipses associées aux différentes boucles donnent les modes d'assemblage. Le nombre de points d'intersection peut être plus grand que un et cette caractéristique du mécanisme est analysée.

Mots-clé: mécanisme parallèle entraîné par câbles, boucle cinématique, statique, singularités.

1 INTRODUCTION

Cable-driven parallel mechanisms are parallel mechanisms in which a moving platform is driven by a number of cables. Such mechanisms have been studied in the recent literature because of their obvious advantages in terms of small moving mass and large range of motion. Pioneer designs of cable-driven parallel mechanisms include the NIST Robocrane [1], the Falcon high-speed parallel manipulator [2] and the Skycam [3].

Several challenging problems arise in the analysis and design of cable-driven parallel mechanisms such as the determination of the workspace, the determination of the wrench capabilities and the computation of the optimal force distribution (see for instance [4, 5, 6, 7]). Indeed, because cables can only work in tension, cable-driven parallel mechanisms are often redundantly actuated, thereby leading to infinitely many solutions to the inverse statics or dynamics problem.

Several practical issues also need to be considered in the design and control of cable-driven parallel mechanisms. In a typical cable-driven parallel mechanism, cables are wound on actuated spools and the extension of the cables is determined using an encoder mounted on the spool. This approach leads to inaccuracies because the ratio between the rotation of the spool and the extension of the cable is generally not constant and depends on how much cable is wound on the spool. Also, it was shown that the tension in the cable at the time of winding may also affect the winding and hence the above mentioned ratio [9].

Given the above limitations, it is proposed here to build a planar cable-driven parallel mechanism based on closed cable loops. By replacing the cable and spool arrangement with closed cable loops, the difficulties of measuring the extention of the cables are alleviated. Also, the stability of the platform may be improved by increasing the number of cables attached to the platform. This paper presents the application of this concept to a planar two-degree-of-freedom parallel mechanism. The mechanism is first introduced and its mechanical design is described. Then the inverse kinematic problem is solved and the velocity equations are derived. Two Jacobian matrices are obtained and a singularity analysis is then performed. A static analysis is presented, based on the principle of virtual work and the wrench capabilities of the mechanism are discussed. Finally, a geometric analysis is presented in order to support the results of the preceding sections.

2 DESCRIPTION OF THE MECHANISM

The structure of a 3-cable 2-dof cable driven parallel mechanism is shown in Fig.(1). There are three cable loops in this mechanism. Each cable is controlled by a slider, passes around two fixed pulleys and then attaches to the end-effector. The position of the end-effector can be changed by controlling the motion of the sliders.

The fixed pulleys are represented by A_{ij}, $i = 1, \ldots, 3$, $j = 1, 2$, the sliders are represented by B_i, $i = 1, \ldots, 3$. The location of point A_{ij}, $i = 1, \ldots, 3$, $j = 1, 2$ is known and expressed as $\mathbf{r}_{Aij} = [x_{Aij}, y_{Aij}]^T$, $i = 1, \ldots, 3$, $j = 1, 2$. The respective length of loops $PA_{11}B_1A_{12}P$, $PA_{21}B_2A_{22}P$ and $PA_{31}B_3A_{32}P$ is L_i, $i = 1, \ldots, 3$. The direction of motion of the sliders is noted $\mathbf{s}_i = [x_{si}, y_{si}]^T$, $\mathbf{s}_i^T \mathbf{s}_i = 1$, $i = 1, \ldots, 3$ and the sliding guides pass through points R_i, $\mathbf{r}_{Ri} = [x_{Ri}, y_{Ri}]^T$, $i = 1, \ldots, 3$. Then, the position of point B_i, noted $\mathbf{r}_{Bi} = [x_{Bi}, y_{Bi}]^T$, $i = 1, \ldots, 3$ can be expressed as

$$\mathbf{r}_{Bi} = \mathbf{r}_{Ri} + \rho_i \mathbf{s}_i, \quad i = 1, \ldots, 3 \tag{1}$$
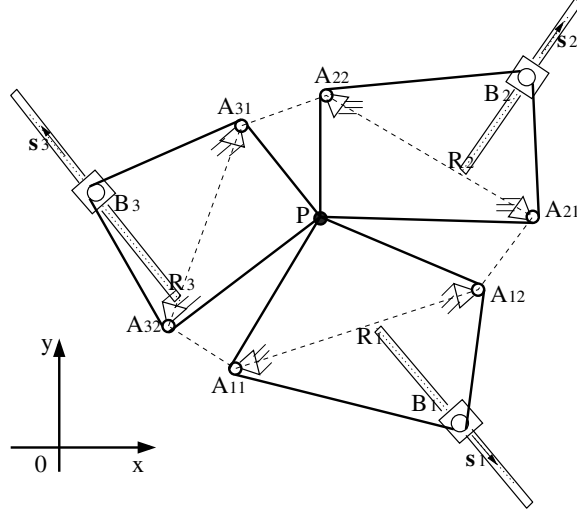
Figure 1: Schematic representation of a 3-cable 2-dof cable driven parallel mechanism.

where ρ_i represents the extension of the ith slider, i.e., the ith joint coordinate.

3 INVERSE KINEMATICS

The solution of the inverse kinematic problem consists in determining the actuator coordinates ρ_i for a given position of the end-effector P, given as $\mathbf{r}_p[x_p, y_p]^T$. From the geometry of the ith cable loop, the total loop length, L_i, can be written as

$$\mid \mathbf{r}_p - \mathbf{r}_{Ai1} \mid + \mid \mathbf{r}_p - \mathbf{r}_{Ai2} \mid + \mid \mathbf{r}_{Ai1} - \mathbf{r}_{Bi} \mid + \mid \mathbf{r}_{Ai2} - \mathbf{r}_{Bi} \mid = L_i, \quad i = 1, \dots, 3. \tag{2}$$

Expanding eq.(2), we obtain

$$C_{1i}\rho_i^2 + C_{2i}\rho_i + C_{3i} = 0, \quad i = 1, \dots, 3 \tag{3}$$

where

$l_i = L_i - \mid \mathbf{r}_p - \mathbf{r}_{Ai1} \mid - \mid \mathbf{r}_p - \mathbf{r}_{Ai2} \mid$
$C_{1i} = 4 \left[l_i^2 - \left(\mathbf{r}_{Ai2}^T \mathbf{s}_i - \mathbf{r}_{Ai1}^T \mathbf{s}_i \right)^2 \right]$
$C_{2i} = 4 \left[2l_i^2 \left(\mathbf{r}_{Ri}^T \mathbf{s}_i - \mathbf{r}_{Ai1}^T \mathbf{s}_i \right) - 4 \left(\mathbf{r}_{Ai2}^T \mathbf{s}_i - \mathbf{r}_{Ai1}^T \mathbf{s}_i \right) \left(l_i^2 + \mathbf{r}_{Ai1}^T \mathbf{r}_{Ai1} - \mathbf{r}_{Ai2}^T \mathbf{r}_{Ai2} + 2\mathbf{r}_{Ai2}^T \mathbf{r}_{Ri} - 2\mathbf{r}_{Ai1}^T \mathbf{r}_{Ri} \right) \right]$
$C_{3i} = 4l_i^2 \left(\mathbf{r}_{Ai1}^T \mathbf{r}_{Ai1} + \mathbf{r}_{Ri}^T \mathbf{r}_{Ri} - 2\mathbf{r}_{Ai1}^T \mathbf{r}_{Ri} \right) - l_i^4 - \left(\mathbf{r}_{Ai1}^T \mathbf{r}_{Ai1} - \mathbf{r}_{Ai2}^T \mathbf{r}_{Ai2} + 2\mathbf{r}_{Ai2}^T \mathbf{r}_{Ri} - 2\mathbf{r}_{Ai1}^T \mathbf{r}_{Ri} \right)^2$
$\quad - 2l_i^2 \left(\mathbf{r}_{Ai1}^T \mathbf{r}_{Ai1} - \mathbf{r}_{Ai2}^T \mathbf{r}_{Ai2} + 2\mathbf{r}_{Ai2}^T \mathbf{r}_{Ri} - 2\mathbf{r}_{Ai1}^T \mathbf{r}_{Ri} \right)$

Therefore, the inverse kinematic problem can be solved by computing the roots of eq.(3). It can be observed that two solutions are obtained for each cable loop which leads to 8 solutions for the complete mechanism

4 VELOCITY EQUATIONS AND JACOBIAN MATRICES

Differentiating eq.(2) with respect to time and collecting terms, we can get

$$
\begin{bmatrix} (\mathbf{u}_{11} + \mathbf{u}_{12})^T \\ (\mathbf{u}_{21} + \mathbf{u}_{22})^T \\ (\mathbf{u}_{31} + \mathbf{u}_{32})^T \end{bmatrix} \begin{bmatrix} \dot{x}_p \\ \dot{y}_p \end{bmatrix} = \begin{bmatrix} (\mathbf{v}_{11} + \mathbf{v}_{12})^T \mathbf{s}_1 & 0 & 0 \\ 0 & (\mathbf{v}_{21} + \mathbf{v}_{22})^T \mathbf{s}_2 & 0 \\ 0 & 0 & (\mathbf{v}_{31} + \mathbf{v}_{32})^T \mathbf{s}_3 \end{bmatrix} \begin{bmatrix} \dot{\rho}_1 \\ \dot{\rho}_2 \\ \dot{\rho}_3 \end{bmatrix}
\tag{4}
$$

where

$$
\mathbf{u}_{ij} = \frac{\mathbf{r}_p - \mathbf{r}_{Aij}}{\mid \mathbf{r}_p - \mathbf{r}_{Aij} \mid}, \quad i = 1, \dots, 3, \quad j = 1, 2
$$

$$
\mathbf{v}_{ij} = \frac{\mathbf{r}_{Aij} - \mathbf{r}_{Bi}}{\mid \mathbf{r}_{Aij} - \mathbf{r}_{Bi} \mid}, \quad i = 1, \dots, 3, \quad j = 1, 2.
$$

In other words, eq.(4) can be writen as:

$$
\mathbf{J}_x \dot{\mathbf{x}} = \mathbf{J}_\rho \dot{\mathbf{q}}
\tag{5}
$$

where the two Jacobian matrices given in eq.(4) are noted $\mathbf{J}_x$ and $\mathbf{J}_\rho$.

5 SINGULARITY ANALYSIS

The configurations of the mechanism that lead to $det(\mathbf{J}_\rho) = 0$ or $det(\mathbf{J}_x^T \mathbf{J}_x) = 0$ are singular configurations.

For $det(\mathbf{J}_\rho) = 0$, we get:

$$
\mathbf{s}_i^T (\mathbf{v}_{i1} + \mathbf{v}_{i2}) = 0, \quad i = 1, \dots, 3.
\tag{6}
$$

From eq.(6), we can find the corresponding value of ρ_i, namely

$$
\rho_i = \mathbf{s}_i^T \mathbf{m}_i
\tag{7}
$$

where

$$
\mathbf{m}_i = \begin{bmatrix} \dfrac{(x_{Ai1} - x_{Ri}) \mid \mathbf{r}_{Ai2} - \mathbf{r}_{Bi} \mid}{\mid \mathbf{r}_{Ai1} - \mathbf{r}_{Bi} \mid + \mid \mathbf{r}_{Ai2} - \mathbf{r}_{Bi} \mid} + \dfrac{(x_{Ai2} - x_{Ri}) \mid \mathbf{r}_{Ai2} - \mathbf{r}_{Bi} \mid}{\mid \mathbf{r}_{Ai1} - \mathbf{r}_{Bi} \mid + \mid \mathbf{r}_{Ai2} - \mathbf{r}_{Bi} \mid} \\ \dfrac{(y_{Ai1} - y_{Ri}) \mid \mathbf{r}_{Ai2} - \mathbf{r}_{Bi} \mid}{\mid \mathbf{r}_{Ai1} - \mathbf{r}_{Bi} \mid + \mid \mathbf{r}_{Ai2} - \mathbf{r}_{Bi} \mid} + \dfrac{(y_{Ai2} - y_{Ri}) \mid \mathbf{r}_{Ai2} - \mathbf{r}_{Bi} \mid}{\mid \mathbf{r}_{Ai1} - \mathbf{r}_{Bi} \mid + \mid \mathbf{r}_{Ai2} - \mathbf{r}_{Bi} \mid} \end{bmatrix}
$$

By inspection of the above equations, it is clear that if the direction of $\mathbf{s}_i$ is perpendicular to the line $A_{i1}A_{i2}$, i.e., $\mathbf{s}_i \perp (\mathbf{v}_{i1} + \mathbf{v}_{i2})$ such singularity points are easily avoided.

For $det(\mathbf{J}_x^T \mathbf{J}_x) = 0$, it is more difficult to obtain a singularity equation. However, by inspection of eq.(4) it is clear that the singularities occur when eqs.(8), (9) and (10) are all satisfied, i.e.,

$$
det \left(\begin{matrix} (\mathbf{u}_{11} + \mathbf{u}_{12})^T \\ (\mathbf{u}_{21} + \mathbf{u}_{22})^T \end{matrix} \right) = 0
\tag{8}
$$

$$
det \left(\begin{matrix} (\mathbf{u}_{11} + \mathbf{u}_{12})^T \\ (\mathbf{u}_{31} + \mathbf{u}_{32})^T \end{matrix} \right) = 0
\tag{9}
$$

$$det\left(\begin{array}{c}(\mathbf{u}_{21}+\mathbf{u}_{22})^T \\ (\mathbf{u}_{31}+\mathbf{u}_{32})^T\end{array}\right)=0. \tag{10}$$

Fig.(2) shows an example of the loci associated with eqs.(8), (9) and (10). The solid curve is the solution of each equation. We can see that the three curves do not have a common intersection point. Actually, in practice, it is easy to design the mechanism such that the singularities corresponding to $det(\mathbf{J}_x^T\mathbf{J}_x)=0$ do not exist.
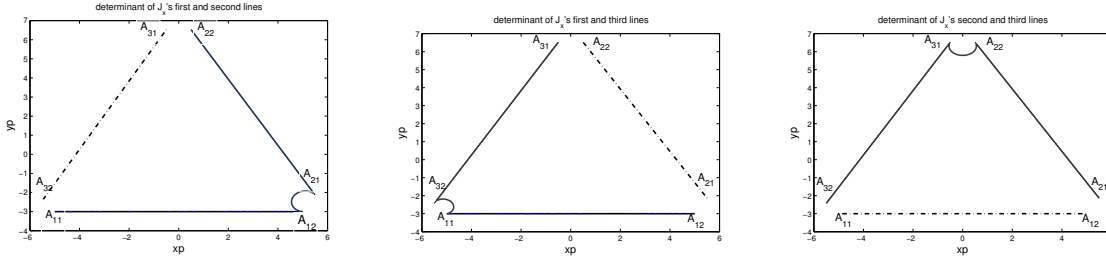
Figure 2: Loci corresponding to eqs.(8), (9) and (10).

6 STATIC ANALYSIS
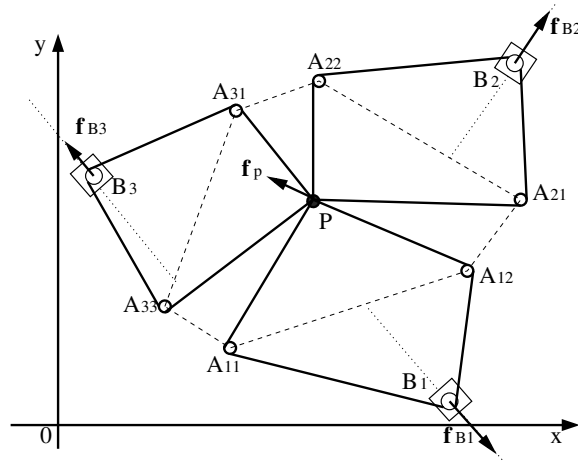
Figure 3: Actuation and platform forces for the 3-cable 2-dof cable driven parallel mechanism.

The forces acting on the 3-cable 2-dof cable driven parallel mechanism are shown in fig.(3). The actuator forces are $\mathbf{f}_{Bi}$, $i=1,\ldots,3$. According to the kinematic model mentioned earlier, the directions of the actuating forces are $\mathbf{s}_i$, $i=1,\ldots,3$. The external force at the end-point is $\mathbf{f}_p=[f_x,f_y]^T$. As a whole system, the mechanism should be balanced with $\mathbf{f}_{Bi}$, $i=1,\ldots,3$ and $\mathbf{f}_p$. Using the principle of virtual work, we can get

$$\mathbf{f}_{B1}^T\delta\mathbf{r}_{B1}+\mathbf{f}_{B2}^T\delta\mathbf{r}_{B2}+\mathbf{f}_{B3}^T\delta\mathbf{r}_{B3}+\mathbf{f}_p^T\delta\mathbf{r}_p=0 \tag{11}$$

Substituting eq.(1) into eq.(11), one then obtains

$$\mathbf{f}_{B1}^T \mathbf{s}_1 \delta\rho_1 + \mathbf{f}_{B2}^T \mathbf{s}_2 \delta\rho_2 + \mathbf{f}_{B3}^T \mathbf{s}_3 \delta\rho_3 + \mathbf{f}_p \delta\mathbf{r}_p = 0. \tag{12}$$

Eq.(12) can be written as

$$-\mathbf{f}_B^T \delta\boldsymbol{\rho} = \mathbf{f}_p^T \delta\mathbf{r}_p \tag{13}$$

where

$$\mathbf{f}_B = \begin{bmatrix} \mathbf{f}_{B1}^T \mathbf{s}_1 & \mathbf{f}_{B2}^T \mathbf{s}_2 & \mathbf{f}_{B3}^T \mathbf{s}_3 \end{bmatrix}^T, \quad \delta\boldsymbol{\rho} = \begin{bmatrix} \delta\rho_1 & \delta\rho_2 & \delta\rho_3 \end{bmatrix}^T$$

in which $\delta\boldsymbol{\rho}$ and $\delta\mathbf{r}_p$ are respectively virtual changes of the positions of the sliders and the virtual generalized displacement of the end-effector. From eq.(4), we have

$$\delta\boldsymbol{\rho} = \mathbf{J}_\rho^{-1} \mathbf{J}_x \delta\mathbf{r}_p$$

and substituting into eq.(13), we get the static equation:

$$\mathbf{f}_p = -\mathbf{J}_x^T \mathbf{J}_\rho^{-T} \mathbf{f}_B. \tag{14}$$

7 WRENCH CAPABILITIES OF THE MECHANISM

The static equation expressing the relationship between the actuator forces and the external force applied at the end-effector can be rewritten as

$$\mathbf{W}\mathbf{f}_B = \mathbf{f}_p \tag{15}$$

where

$$\mathbf{W} = -\mathbf{J}_x^T \mathbf{J}_\rho^{-T}.$$

Assuming that the minimun slider force and the maximun slider force are known, then the available wrench set at the platform can be expressed as

$$A = \left\{ \mathbf{f}_p \in \mathbb{R}^2 \mid \mathbf{f}_p = \sum_{i=1}^{3} \beta_i \mathbf{w}_i + \mathbf{W}\mathbf{f}_{Bmin}, \quad 0 \le \beta_i \le (\mathbf{f}_{Bmax} - \mathbf{f}_{Bmin}) \right\}. \tag{16}$$

where $\mathbf{w}_i$ is the ith column of matrix $\mathbf{W}_i$

For instance, if the minimum slider force is $\mathbf{f}_{Bmin} = (1,1,1)^T$, the maximum slider force is $\mathbf{f}_{Bmax} = (10,10,10)^T$, and if the geometry of the mechanism is such that the pulleys are located by pairs at points $(-6,0)$, $(6,0)$, $(0,6\sqrt{3})$, then the available wrenches are easily determined. They are the convex hull of the extreme wrenches, as given in eq.(16). Two examples are illustrated for the above parameters in figs. 4 and 5.
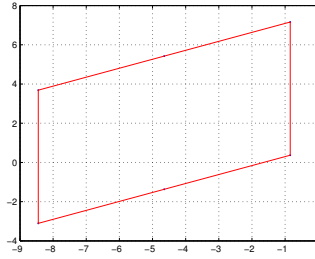
Figure 4: Available wrench set when the end effector is located at $(0, 3\sqrt{3})$.
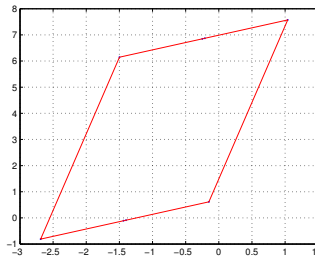
Figure 5: Available wrench set when the end effector at $(2, 3\sqrt{3})$.

8 GEOMETRIC ANALYSIS

Roughly speaking, the end point of this mechanism can reach any point in the polygon formed by vertices $A_{11}A_{12}A_{21}A_{22}A_{31}A_{32}A_{11}$. However, there are some points that can cause the cable loops to become loose. Indeed, for a given value of ρ_i, for one cable loop, the trajectory of the end-point is a portion of ellipse. The intersection of the three ellipses gives the position of the end point. Depending on how the ellipses intersect, some of the cables may become slack. This is illustrated in fig.6.

For a given point of the workspace, using the equations of the ellipses we can find out whether the cables will become loose or not. However, it is much more meaningful to determine the regions in which the cables can become loose using an approach based on geometry.

Since in a given loop the cable can move freely around the pulleys (all pulleys are free to rotate), the tension in the cable must be the same everywhere (if friction in the pulleys is neglected). Therefore, the tension in each of the two cable ends of a given loop attached to the platform must be the same.

Considering the geometric construction of fig.(7), the following vectors are defined:

$$\begin{aligned}
\mathbf{u}_1 &= \mathbf{u}_{11} + \mathbf{u}_{12} \\
\mathbf{u}_2 &= \mathbf{u}_{21} + \mathbf{u}_{22} \\
\mathbf{u}_3 &= \mathbf{u}_{31} + \mathbf{u}_{32}.
\end{aligned} \tag{17}$$
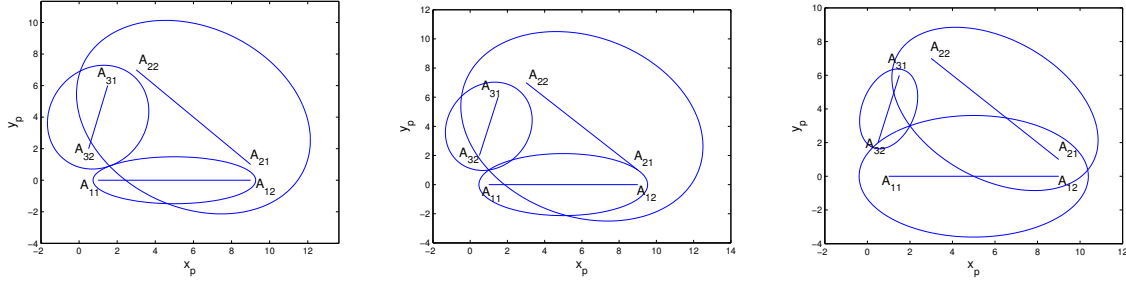
Figure 6: Intersection of the three ellipses associated with the cable loops.
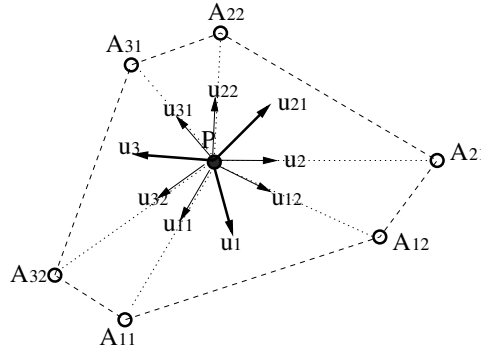
Figure 7: Definition of the direction of the force vectors.

Clearly, the force applied to the platform by the ith cable loop must be in the direction of vector $\mathbf{u}_i$. To avoid a situation in which one of the cables becomes loose, vectors $\mathbf{u}_i, i = 1, ..., 3$ must be in a force-closed configuration. The boundary of this region is reached when two of the $\mathbf{u}_i, i = 1, ..., 3$ are aligned. Therefore, the equation describing this boundary is the combination of eq.(8), eq.(9) and eq.(10).

The solution of eq.(8), eq.(9) and eq.(10) leads to two possible situations. One situation is that one of the rows is zero, the other situation is that the direction of each row is along the same line. The segment between the pulleys of line $A_{11}A_{12}$, $A_{21}A_{22}$, $A_{31}A_{32}$ corresponds to the first situation. The second situation is the solution of eq.(18), for eq.(8) $i = 1$, $j = 2$, for eq.(9) $i = 1$, $j = 3$, and for eq.(10) $i = 2$, $j = 3$.

$$\begin{aligned}
&\sqrt{A_{i2}}\sqrt{A_{j2}}\left[(y_{ai1} - y_{aj1})x_p + (x_{aj1} - x_{ai1})y_p + x_{ai1}y_{aj1} - x_{aj1}y_{ai1}\right] \\
&+\sqrt{A_{i2}}\sqrt{A_{j1}}\left[(y_{ai1} - y_{aj2})x_p + (x_{aj2} - x_{ai1})y_p + x_{ai1}y_{aj2} - x_{aj2}y_{ai1}\right] \\
&+\sqrt{A_{i1}}\sqrt{A_{j2}}\left[(y_{ai2} - y_{aj1})x_p + (x_{aj1} - x_{ai2})y_p + x_{ai2}y_{aj1} - x_{aj1}y_{ai2}\right] \\
&+\sqrt{A_{i1}}\sqrt{A_{j1}}\left[(y_{ai2} - y_{aj2})x_p + (x_{aj2} - x_{ai2})y_p + x_{ai2}y_{aj2} - x_{aj2}y_{ai2}\right] = 0
\end{aligned} \qquad (18)$$

where

$$A_{ik} = (x_p - x_{aik})^2 + (y_p - y_{aik})^2 \quad k = 1, 2$$

One example of the boundary of the force-closed configurations is shown Fig.(8).
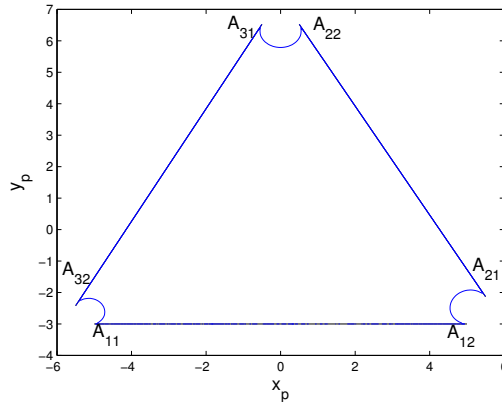
Figure 8: Boundary of the force-closed region for the 3-cable 2-dof cable driven parallel mechanism.

9 CONCLUSIONS

This paper presented a 3-cable 2-DOF closed-loop cable-driven parallel mechanism. The cables form loops that are free to move around a set of free pulleys. Each cable loop is attached to the end-effector. The position of the end-effector is controlled using sliders that displace one of the pulleys along an axis. This architecture has the advantage of eliminating the need to wind cables around a spool.

The inverse kinematics, the Jacobian matrices and the static equations were determined. The singularities of the mechanism have been analyzed based on the two Jacobian matrices. Also, using the method presented in [7], the set of available wrenches was obtained from the static equations.

Finally, a special geometric characteristic of the novel architecture was studied. It was observed that, for a given position of the ith slider, the trajectory of the end-point of the ith cable loop is a portion of ellipse. The intersection of the ellipses gives the position of the end point. From geometric reasoning, the boundary of the force-closed workspace was determined.

10 ACKNOWLEDGEMENTS

REFERENCES

[1] Albus, J., Bostelman, R., and Dagalakis, N., 'The NIST Robocrane,' Journal of Robotics Systems, Vol. 10, No. 5, pp. 709–724, 1993.

[2] Kawamura, S., Choe, W., Tanaka, S., and Pandian, S., 'Development of an ultrahigh speed robot FALCON using wire drive system,' in Proceedings of the IEEE International Conference on Robotics and Automation, Vol. 1, pp. 215–220, Nagoya, Japan, 1995.

[3] Cone, L. L., 'Skycam, an aerial robotic camera sys- tem,' Byte, Vol. 10, pp. 122–132, 1985.

[4] Stump, E. and Kumar, V., 'Workspace Delienation of Cable-Actuated Parallel Manipulators,' in Proceedings of the ASME International Design Engineering Technical Conferences, Mechanisms and Robotics Conference, Salt Lake City, USA, 2004.

[5] Bosscher, P. and Ebert-Uphoff, I., 'Wrench-based analysis of cable-driven robots,' in Proceedings of the IEEE International Conference on Robotics and Automation, Vol. 5, pp. 4950–4955, New Orleans, USA, 2004.

[6] Gouttefarde, M., Merlet, J., and Daney, D., 'Wrench-feasible workspace of parallel cable-driven mechanisms,' in Proceedings of the IEEE International Conference on Robotics and Automation, pp. 1492–1497, Rome, Italy, 2007.

[7] Bouchard, S., Gosselin, C. and Moore, B., 'On the ability of a cable-driven robot to generate a prescribed set of wrenches,' in Proceedings of the ASME International Design Engineering Technical Conferences, Mechanisms and Robotics Conference, Brooklyn, New York, USA, DETC2008-49518, 2008.

[8] Garg, V., Nokleby, S.B. and Carretero, J.A., 'Force-moment capabilities of redundantly-actuated spatial parallel manipulators using two methods,' in Proceedings of the CCToMM Symposium on Mechanisms, Machines, and Mechatronics, May 31–June 1, St-Hubert, Québec, 2007.

[9] Gosselin, C., Poulin, R. and Laurendeau, D., 'A planar parallel 3-dof cable-driven haptic interface,' Proceedings of the 12th World Multi-Conference on Systemics, Cybernetics and Informatics: WM-SCI '08, Orlando, Florida, USA, June 29 – July 2, Vol. 3, pp. 266–271, 2008.